Available online at www.sciencedirect.com
SCIENCE DIRECT
Journal of Power Sources 158 (2006) 779–783
JOURNAL OF POWER SOURCES
www.elsevier.com/locate/jpowsour

Synthesis of the CoOOH fine nanoflake film with the high rate capacitance property

Eiji Hosono [a], Shinobu Fujihara [b], Iraru Honma [a], Masaki Ichihara [c], Haoshen Zhou [a,*]

[a] *National Institute of Advanced Industrial Science and Technology, Umezono, 1-1-1, Tsukuba 305-8568, Japan*
[b] *Keio University, 3-14-1, Hiyoshi, Kohoku-ku, Yokohama 223-8522, Japan*
[c] *Material Design and Characterization Laboratory, Institute for Solid State Physics, University of Tokyo, 5-1-5, Kashiwanoha, Kashiwa, Chiba 277-8581, Japan*

Received 23 August 2005; received in revised form 15 September 2005; accepted 19 September 2005
Available online 21 November 2005

Abstract

The CoOOH film on the nickel foil is fabricated via layered hydroxide cobalt acetate (LHCA) film with nanosheets morphology, which is synthesized by chemical bath deposition method. The LHCA nanosheets film is converted into CoOOH fine nanoflake films with high porous and high surface area by the oxidation reaction based on the dissolved oxygen in KOH solution. The intercalated acetate into the LHCA layer, which is strong basic species, caused the oxidation. The electrochemical capacitance property of the resultant CoOOH fine nanoflake film is studied by cyclic voltammetry (CV). In the CV, a good high rate property is indicated by the results of CV at high rate scan. It is caused by the specific morphology of the CoOOH fine nanoflake films.

Keywords: CoOOH; Electrochemical capacitor; High rate property; Chemical bath deposition

1. Introduction

An electrochemical capacitors based on the electric double layer (EDLC) is suitable for a high power energy storage system, which could be used for the hybrid electric vehicles (HEV). Moreover, the electrochemical capacitors with pseudo-capacitance such as RuO_2, IrO_2, and NiO have been focused in recent years because those capacitors have larger energy density than that of EDLC [1–3]. The cobalt compounds capacitors including, CoO_x, Co_3O_4, and $Co(OH)_2$ are also studied for the same reason [4–6].

In order to fabricate the high power energy storage device, the synthesis of nanoparticle and high porous materials is an important point because the high surface area produces the large reaction place and a lot of pores cause rapid transfer of the electrolyte [7]. The metal oxide films via metal hydroxide [8–11], which is directly synthesized on the substrate by chemical bath deposition (CBD), are suitable for the electrochemical devices because the micro- and nanostructure film with high surface area and high porous morphology is easily obtained. In processes of synthesizing metal oxide powders, nanostructural material design as film is generally difficult to accomplish because heating at high temperatures is necessary for fixing of the powder on the substrate as the films. During high-temperature processes, the sintering and/or aggregation of nanosized metal oxide grains can occur, leading to loss of nanostructural features. Generally, the CBD has been utilized for preparing various kinds of metal oxides and sulfides because thin-film materials can be fabricated at low temperatures without expensive and special apparatus required for vapor-phase techniques [12]. The chemical reaction in the solution produces less soluble chemical species and causes a low degree of supersaturation of the solutions, which results in heterogeneous nucleation on foreign substrates [13]. The most important aspect of the CBD is the preservation of low degrees of supersaturation. High degrees of supersaturation induce homogeneous nucleation rather than the film formation. Thus the CBD process is promising as unique chemical routes to produce nanostructured films in a "soft" manner. Metal hydroxide compounds, expressed by layered hydroxide metal salts (LHMSs) in a general formula of $M_x(OH)_y(X)_z \cdot nH_2O$ (M: metal, X: anion),

* Corresponding author. Tel.: +81 298 61 5795; fax: +81 298 61 5829/5799.
E-mail address: hs.zhou@aist.go.jp (H. Zhou).

0378-7753/$ – see front matter © 2005 Elsevier B.V. All rights reserved.
doi:10.1016/j.jpowsour.2005.09.052

can be also synthesized by CBD process [14–16]. Morphologies of these materials are characterized by nanosheets morphology based on their layered crystal structure. Pyrolysis of nanostructured metal hydroxide results in nanostructured metal oxides, which have large surface area without microstructural deformation. So, LHMSs can be used as "self-templates" for producing nanostructural metal oxide films because the nanosheets morphology is similar to LHMSs films [8–11].

Here, we show the solution synthesis of CoOOH film on the nickel foil via LHCA film by the CBD process. On the surface facing the bottom of the bottle (under side), the LHCA thin film constructed by nanosheets is fabricated and the thick film constructed by aggregated nanosheets is foamed on the top side of the nickel foil surface. In this work, we never conducted the heat treatment for pyrolysis and oxidation reaction to obtain the CoOOH films on the substrate. The LHCA film is converted into CoOOH by oxidation due to the dissolved oxygen in the KOH solution. The nanosheets morphology is changed to the fine nanoflake morphology with a large surface area. Generally, CoOOH is known as the high conductive materials of 5 S cm^{-1} [17–19]. Hence, the capacitor property using this CoOOH fine nanoflake film indicates good high rate property based on the high surface area, a lot of mesopores and good electronic conductivity.

2. Experimental

Solutions for the CBD process were prepared by dissolving $Co(CH_3COO)_2{\cdot}4H_2O$ (99.9% purity, Wako Pure Chemicals Co., Ltd.) in methanol/water mixed solution. The volume ratio of water/methanol was 4:1. A concentration of metal ions was adjusted to 0.15 mol $d m^{-3}$. Nickel foil was used as substrates for the deposition. The nickel foils were put into bottles filled with the solutions and sealed up, then were kept at 60 °C for 12 h in a drying oven. After the deposition, the LHCA films were rinsed by ethanolic solution (ethanol:methanol:water = 95:5:5) and were dried at room temperature. The LHCA films were put into bottles filled with the 1.0 M KOH solutions and sealed up, and were kept at room temperature for 12 h. The LHCA films were converted into CoOOH.

The crystal structure was identified by X-ray diffraction (XRD) analysis using Cu Kα radiation in the 2θ range 5–80°. The morphology was observed by field emission scanning electron microscopy (FESEM) and high-resolution transmission electron microscopy (HRTEM). The specific surface area was estimated by the BET method based on the N_2 adsorption.

For electrochemical measurement, the fabricated CoOOH film on the nickel foil was used as working electrode. The reference and counter electrode were SCE electrode and titanium mesh, respectively. A 1 mol $d m^{-3}$ KOH aqueous solution was used as electrolyte.

3. Results and discussion

Fig. 1(a) shows XRD patterns of the powder, which is obtained by mixing the scratched film from the surface facing the bottom of the bottle and precipitated film on the opposite surface, after immersion in the precursor solution at 60 °C for 12 h. In Fig. 1(a), the first three diffraction peaks in lower diffraction angles are explained as (0 0 3), (0 0 6) and (0 0 9) of layered hydroxide cobalt acetate $(Co(OH)_{2-x}(Ac)_x{\cdot}nH_2O$ with (x, n) in a range of (0.38–0.50, 0.53–0.50) having features typical of incompletely ordered lamellar compounds related to brucite type layers [14,20].

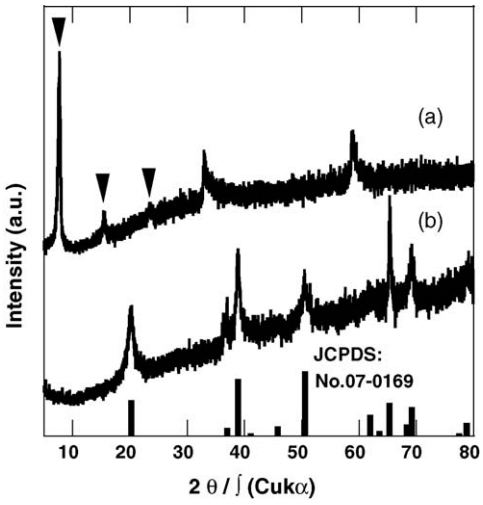

Fig. 1. XRD patterns of the (a) LHCA and (b) CoOOH films. The measurement is conducted by using those powders, which are scratched from the nickel foil.

Fig. 1(b) shows XRD patterns of the film obtained by the immersion of LHCA film into the 1 M KOH solution for 12 h. The film is scratched from the substrate after the immersion in the KOH solution. All the diffraction peaks agree with those of CoOOH form (JCPDS: No. 07-0169). So, the LHCA with Co^{2+} is converted into CoOOH with Co^{3+} by the immersion into the KOH solution. The oxidation from 2+ to 3+ of cobalt in cobalt hydroxide by oxygen in the KOH solution is reported because the stability of Co^{3+} in KOH solution is well known [21]. However, commercial β-$Co(OH)_2$ (JCPDS: No. 45-0031) was not converted into CoOOH in 1 M KOH solution for 12 h. In a word, Co^{2+} is oxidized by oxygen, when the pH is greatly larger than that of 1 M KOH. It is considered that the oxidation in this work using 1 KOH solution is based on intercalated acetate ion in the LHCA because the acetate ion behavior as strong basic species [22] in our previous works. In the paper, Ac^- was produced the similar state to the high pH condition in spite of neutral pH condition because the Ac^- ions can act as a strong base because of the smaller dissociation constant, K_a, of acetic acid. For example, K_a value is as small as 10–9.7 in methanol [23]. Therefore, LHCA is oxidized into CoOOH by dissolved oxygen in the system of 1 M KOH solution with Ac^-, which is similar to the high pH condition.

Fig. 2(a)–(c) are the FE-SEM images of the LHCA films. Fig. 2(a) (top view) and (b) (side view) are the images of the film on the surface facing the bottom of the bottle. Fig. 2(c) is the image of the opposite surface. We can see the vertically grown LHCA nanosheets in Fig. 2(a) and (b), which are grown on the flatly covered LHCA sheet on the substrate due to the concentration gradient. The growth foam is similar to the layered hydroxide zinc acetate and nickel acetate [9,10]. On the other

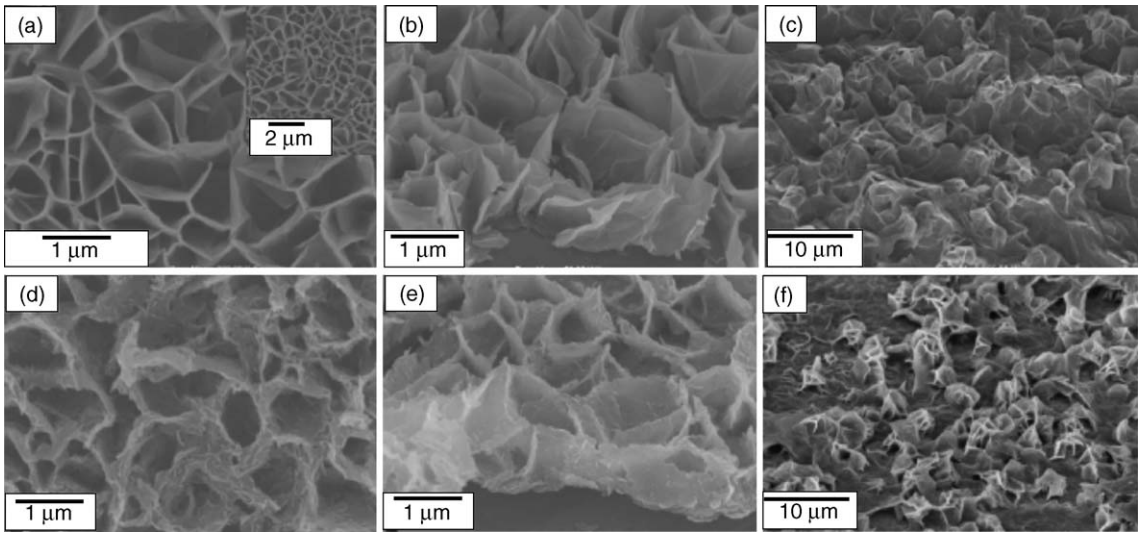

Fig. 2. FE-SEM images of the ((a)–(c)) LHCA and ((d)–(f)) CoOOH film. The images of (a), (b), (d), (e) and (c) and (f) are the film on the surface facing the bottom of the bottle and the opposite surface, respectively.

hands, the aggregated nanosheets on the flatly covered LHCA on the substrate are observed from the images of the top side of the nickel foil as shown in Fig. 2(c). It is considered that the morphology is fabricated as shown in Scheme 1. The aggregated nanosheets, which are formed by homogeneous nucleation, are precipitated on the LHCA covered top side surface based on the heterogeneous nucleation. The resultant morphology based on the homo and heterogeneous nucleation is not similar to that of the surface facing the bottom of the bottle based on only heterogeneous nucleation. Fig. 2(d)–(f) are the FE-SEM images of the CoOOH films. Fig. 2(d) (top view) and (e) (side view) are the images of the film on the surface facing the bottom of the bottle. Fig. 2(f) is the image of the top side surface. The framework of the LHCA nansosheet film in the scale of micrometer is maintained. However, the morphology of each nanosheets in the nanoscale is not maintained. Each LHCA nanosheet is converted into further fine nanoflake. The morphology change of

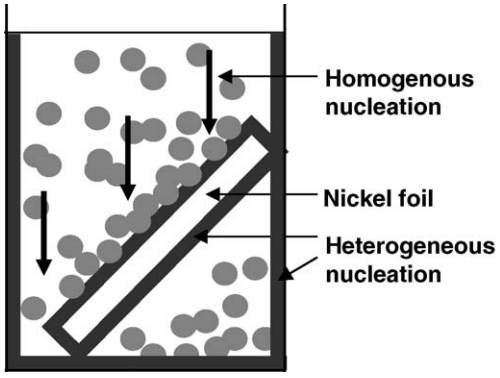

Scheme 1. The model of the film formation by the homogeneous nucleation and the heterogeneous nucleation of the nickel foil in a bottle.

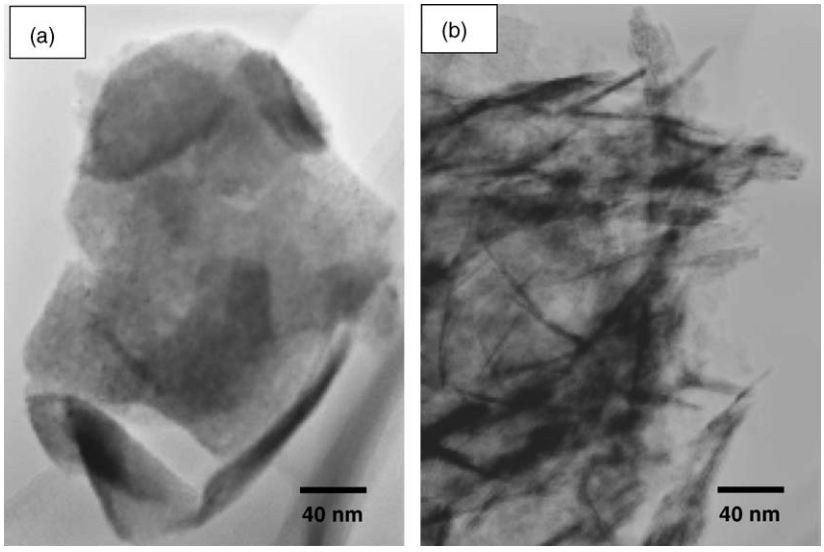

Fig. 3. TEM images of the (a) LHCA and (b) CoOOH films.

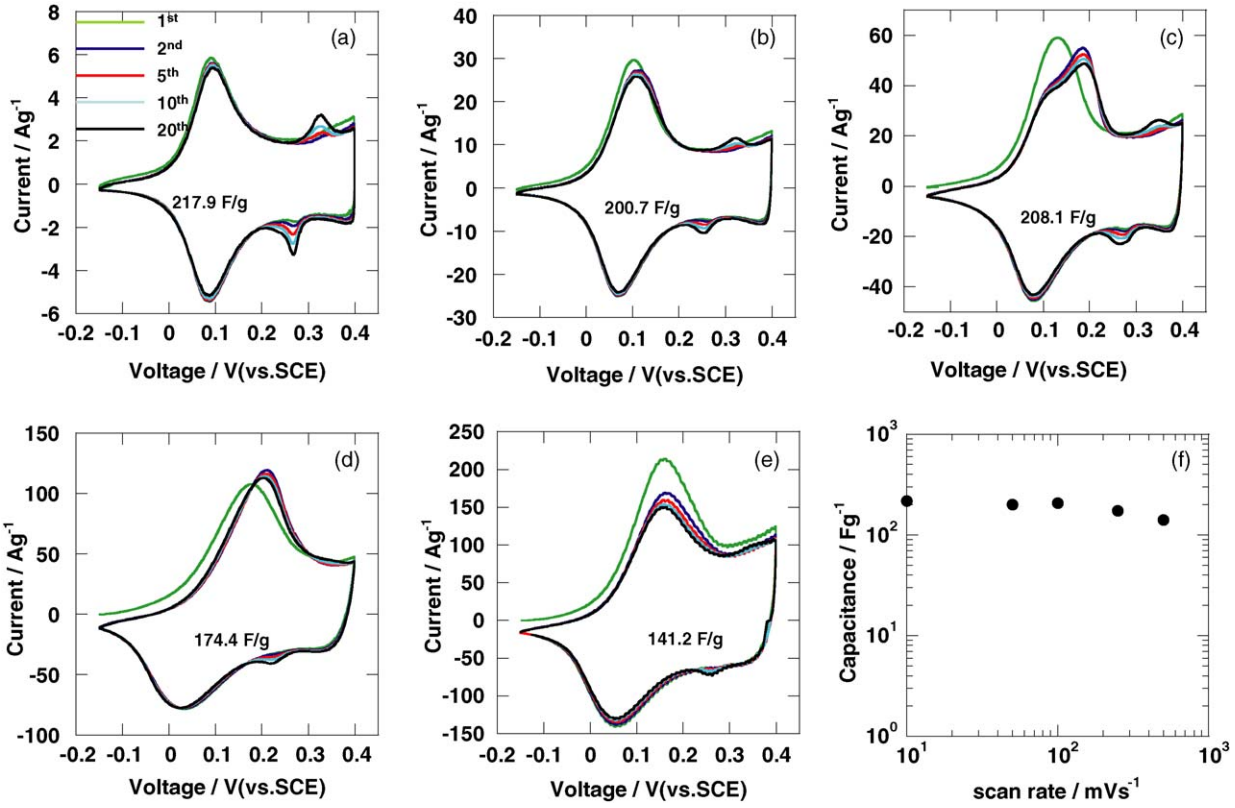

Fig. 4. The CV curves of the CoOOH films by various rate ((a) 10 mV s^{-1}, (b) 50 mV s^{-1}, (c) 100 mV s^{-1}, (d) 250 mV s^{-1}, and (e) 500 mV s^{-1}) and (f) the relationship between capacitance and scan rate. The CV and cycling testing is performed over the voltage range of open-circuit potential (around −0.15 V)–0.4 V vs. SCE reference electrode.

the nanosheet is observed by the TEM as shown in Fig. 3. The image of LHCA nanosheet in Fig. 3(a) indicates the flat sheet structure with thickness of several nm. On the other hands, the CoOOH image in Fig. 3(b) shows the fine nanoflake derived from the LHCA sheet. This fine nanoflake morphology has a high surface area of about 100 m^2 g^{-1}. The porosity of the film, which is estimated by the adsorption isotherm of N_2, is around 65%. The resultant film morphology with the micrometer-scale pores based on the original LHCA structure and nanometer-scale pores due to the CoOOH fine nanoflake is suitable to the electrochemical devices.

The electrochemical properties of CoOOH films are tested via cyclic voltammetry (CV) as shown in Fig. 4. The capacitance is calculated from CV at the 20th cycle. The CV and cycling testing were performed over the voltage range of open-circuit potential (around −0.15 V)–0.4 V vs. SCE reference electrode. The CV curves (10–500 mV s^{-1}) are presented in Fig. 4. All cycles present the cathodic peak at around 0.15 V and the anodic peak at around 0.05 V. In many reports for electrochemical property of $Co(OH)_2$ and Co_3O_4, the potential for electrochemical oxidation and reduction of cobalt compounds are as follows [4,5,24,25].

$$3Co(OH)_2 + 2OH^- \leftrightarrow Co_3O_4 + 4H_2O + 2e^- \quad (0.1\text{–}0.2\ \text{V vs. SCE})$$

$$Co_3O_4 + OH^- + H_2O \leftrightarrow 3CoOOH + e^- \quad (0.1\text{–}0.2\ \text{V vs. SCE})$$

$$CoOOH + OH^- \leftrightarrow CoO_2 + H_2O + e^- \quad (0.4\text{–}0.5\ \text{V vs. SCE})$$

However, in this work, the oxidation from the Co^{2+} to Co^{3+} cannot occur because the CoOOH constructed by only trivalent cobalt is used as starting materials. Bardé et al. reported that the fabrication of $Co_x{}^{4+}Co_{1-x}{}^{3+}OOH$ and the reduction potential from Co^{4+} to Co^{3+} is around 0.1 V (SCE) [26]. It is considered that the redox peaks in Fig. 4 are caused by the reversible electrochemical oxidation and reduction between Co^{3+} and Co^{4+}.

From the all CV curves by various rate from 10 to 500 mV s^{-1}, we can see good cycle property from the first cycle to the 20th cycle. Fig. 4(f) indicates the relationship between capacitance and scan rate. The capacitance around 200 F g^{-1} is not decrease as increasing the rate from 10 to 100 mV s^{-1}. In spite of very high rate of 250 and 500 mV s^{-1}, the capacitances of the 79.1% and 63.6% of that at 10 mV s^{-1} are remained, respectively. Moreover, the relationship between the current peak and scan rate indicate the linear like EDLC. The high electrochemical performance at high scan rate is based on the high conductive nature of CoOOH and morphology control of the micrometer/nanometer scale. The high surface area based on the nanostructure causes the high rate interface reaction between the materials and electrolyte, and microscale structure results in rapidly transfer of electrolyte.

4. Conclusions

We fabricated the electrochemical capacitor with a good high rate performance based on the micro- and nanostructural control

of the CoOOH. The CoOOH film is directly fabricated on the nickel foil via LHCA, which is synthesized by chemical bath deposition. The CoOOH fine nanoflake film is obtained by oxidation of LHCA due to the dissolved oxygen in KOH solution. In this work, electrochemical device with film morphology is obtained by simple solution method without any heating process.

References

[1] J.P. Zheng, P.J. Cygan, T.R. Jow, J. Electrochem. Soc. 142 (1995) 2699.
[2] B.E. Conway, in: F.M. Delnick, M. Tomkiewicz (Eds.), Proceedings on the Symposium on Electrochemical Capacitors, PV 95-29, The Electrochemical Society Proceedings Series, Pennington, NJ, 1995, p. 15.
[3] K.C. Liu, M.A. Anderson, J. Electrochem. Soc. 143 (1996) 124.
[4] C. Lin, J.A. Ritter, B.N. Popov, J. Electrochem. Soc. 145 (1998) 4097.
[5] V. Srinivasan, J.W. Weidner, J. Power Sources 108 (2002) 15.
[6] L. Cao, F. Xu, Y.Y. Liang, H.L. Li, Adv. Mater. 16 (2004) 1853.
[7] H. Zhou, D. Li, M. Hibino, I. Honma, Angew. Chem. Int. Ed. 44 (2005) 797.
[8] E. Hosono, S. Fujihara, I. Honma, H. Zhou, J. Mater. Chem. 15 (2005) 1938.
[9] E. Hosono, S. Fujihara, T. Kimura, H. Imai, J. Colloid Interf. Sci. 272 (2004) 391.
[10] S. Fujihara, E. Hosono, T. Kimura, J. Sol–Gel Sci. Technol. 32 (2004) 165.
[11] E. Hosono, S. Fujihara, I. Honma, H. Zhou, Adv. Mater. 17 (2005) 2091.
[12] T.P. Niesen, M.R. De Guire, J. Electroceram. 6 (2001) 169.
[13] B.C. Bunker, P.C. Rieke, B.J. Tarasevich, A.A. Campbell, G.E. Fryxell, G.L. Graff, L. Song, J. Liu, J.W. Virden, G.L. McVay, Science 264 (1994) 48.
[14] L. Poul, N. Jouini, F. Fiévet, Chem. Mater. 12 (2000) 3123.
[15] R. Rojas, C. Barriga, M.A. Ulibarri, P. Malet, V. Rives, J. Mater. Chem. 12 (2002) 1071.
[16] M. Ogawa, S. Asai, Chem. Mater. 12 (2000) 3253.
[17] P. Benson, G.W.D. Briggs, W.F.K. Wynne-Jones, Electrochim. Acta 9 (1964) 275.
[18] F. Lichtenberg, K. Kleinsorgen, J. Power Sources 62 (2002) 207.
[19] H. Fukunaga, M. Kishimi, T. Ozaki, T. Sakai, J. Electrochem. Soc. 152 (2005) A126.
[20] V. Laget, S. Rouba, P. Rabu, C. Hornick, M. Drillon, J. Magn. Magn. Mater. 154 (1996) L7.
[21] V. Pralong, A. Delahaye-Vidal, B. Gérand, J.M. Tarascon, J. Mater. Chem. 9 (1999) 955.
[22] E. Hosono, S. Fujihara, T. Kimura, H. Imai, J. Sol–Gel Sci. Technol. 29 (2004) 71.
[23] S. Ahrland, in: L.L. Lagowski (Ed.), The Chemistry of Nonaqueous Solvents, vol. VA, Academic Press, New York, 1978, p. 10.
[24] I.G. Casella, M. Gatta, J. Electroanal. Chem. 534 (2002) 31.
[25] M. Longhi, L. Formaro, J. Electroanal. Chem. 464 (2002) 149.
[26] F. Bardé, M.R. Palacin, B. Beaudoin, A. Delahaye-Vidal, J.M. Tarascon, Chem. Mater. 16 (2004) 299.